Positive Pion Scattering from Hydrogen at 24.8 Mev

DOUGLAS MILLER AND JAMES RING
Department of Physics and Astronomy, University of Rochester, Rochester, New York
(Received August 10, 1959)

An angular distribution for the process $\pi^+ + p \rightarrow \pi^+ + p$ has been measured at 24.8 Mev by counter techniques. At this energy the S-wave interaction is larger than the P wave. Differential cross sections at the three center-of-mass angles, 66°, 92°, and 163.5°, are (0.286±0.028) mb/sterad, (0.458±0.042) mb/sterad, and (0.993±0.120) mb/sterad, respectively. Over 250 hydrogen interactions were observed at each angle.

I. INTRODUCTION

PREVIOUS low-energy pion-nucleon scattering measurements have been made by using the cloud chamber,[1] emulsion,[2] or bubble chamber[3] techniques. Now the scintillation counter technique has been extended to 25 Mev. This limit is imposed by the energy loss of the scattered pions in the liquid hydrogen target and detecting counters.

The measurements were made at the 130-in. Rochester synchrocyclotron. A pion beam was produced as the circulating protons reached an aluminum target at full radius. These pions traveled out of the machine through a slot in the shielding to a deflecting magnet and from there to the detecting counters and the liquid hydrogen target.

II. EXPERIMENTAL ARRANGEMENT

A. The pion beam was extracted from the vacuum tank in a trajectory that is shown in Fig. 1. The deflecting magnet and the fringe field of the cyclotron served to select the pion momentum. The energy spectrum immediately before the hydrogen target was characterized by a mean energy of 26 Mev and a half-width at half maximum of 1.6 Mev. In order to obtain this mean energy, it was necessary to use an energy degrader of polyethylene in front of the hydrogen target. A beam intensity of 25 000 positive pions per square inch per minute was obtained. Range measurements determined the energy spectrum and also disclosed the beam contamination fraction. A pulse-height study of the incident beam revealed that positive muons and positrons accounted for this contamination. The positron component was eliminated by discriminating against small pulses.

The angular spread of the beam was measured by using a $\frac{3}{16}$-in. square counter which traversed the beam yielding a beam profile. Such measurements showed the angular spread due to crossfire and multiple scattering (from the polyethylene plug and the counters of the incident telescope) to be less than 4° for all but a negligible percentage of the beam.

B. The liquid hydrogen container was designed to allow demounting of the target cup and of the vacuum container outside the target cup. Each angle then made claim to its own peculiar geometry for the target cup and outside container. The foil thicknesses for the windows varied from 0.0006 to 0.002 inch depending on the geometry and the foil chosen. Foil materials were stainless steel, duralumin or beryllium copper.

C. The scattering geometry had several features which were common to the three angles. Counters 1 and 2 define the incident beam. Counters 3 and 4

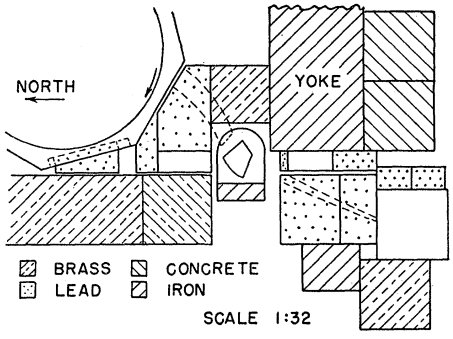

FIG. 1. Plan view of the shielding.

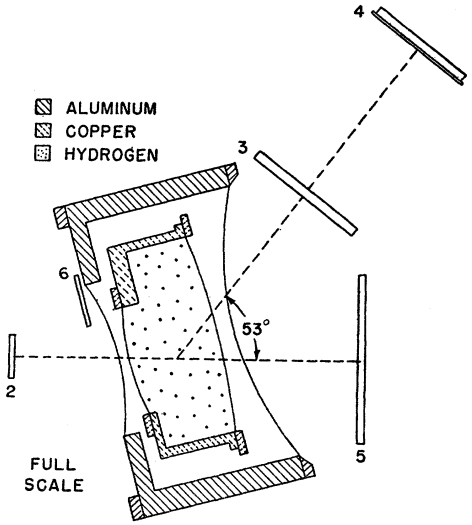

FIG. 2. 53° scattering geometry.

[1] Alston, Von Gierke, Evans, Newport, and Williams, *Proceedings of the* CERN *Symposium on High-Energy Accelerators and Pion Physics, Geneva, 1956* (European Organization of Nuclear Research, Geneva, 1956), p. 237.
[2] Orear, Slater, Lord, Eilenberg, and Weaver, Phys. Rev. **96**, 174 (1954).
[3] Nagle, Hildebrand, and Plano, Phys. Rev. **105**, 718 (1957).

detect the scattered pions, which were analyzed according to pulse height. Counter 5 serves as an anticoincidence detector behind the target.

Figure 2 shows the arrangement of counters and target for the 66° measurement. The counters are all rectangular in shape. Counter 4 defines a solid angle for each point in the illuminated volume of the target. An integration over the volume yields an effective solid angle for this measurement. Counter 6 was inserted in anticoincidence to reject muons produced by decay in flight.

Figure 3 shows the 92° geometry. Counter 4 and the illuminated volume of the target again define the solid angle. The counters are again rectangular, so the solid angle calculation is made in the same manner.

The 163.5° geometry is shown in Fig. 4. Here the counters are either annular or circular. Counter 3 and

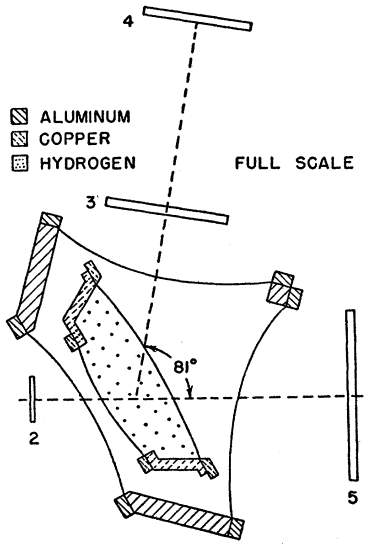

FIG. 3. 81° scattering geometry.

the illuminated volume of the target define the solid angle. Because of the cylindrical geometry the solid angle varies slowly with the radial distance from the beam axis. Therefore, the variation of beam intensity over the target area has a small effect on the determination of the cross section.

D. A block diagram of the electronics is shown in Fig. 5.

The anticoincidence circuit is driven by the 125 rate rather than the large singles counting rate in counter 5. Whenever a $1234\bar{5}$ pulse is recorded, the pulse from counter 3 is displayed on the pulse-height analyzer.

The discriminator is the heart of the coincidence system. Since the space rate of energy loss is so large for 25-Mev pions, discrimination against smaller pulses results in a good signal-to-noise ratio for the scattering experiment. Measurements show greater than 99.9% detection efficiency for such a system.

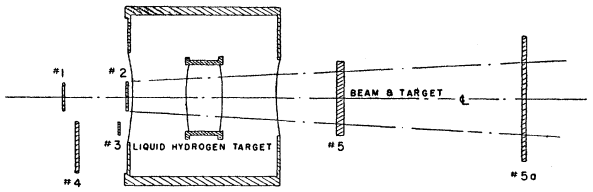

FIG. 4. 160° scattering geometry.

E. Each experimental period included a range curve, a pulse-height analysis of the incident beam, and a measurement of the beam profile. The scattering due to hydrogen was determined from the difference between data taken with the target full and the target empty, but in position. Intermittent checks were made on the detection efficiency by observing the multiple scattering of pions by lead.

III. RESULTS

A. Our uncorrected data are displayed in Table I. Correction factors which were applied to these data appear in Table II. Note that several corrections other than the correction for beam contamination were common to all angles. Other corrections were more important at a particular angle.

At 66°, muon scattering in hydrogen by the Coulomb interaction was indistinguishable from the events of interest. A correction factor of 0.998 ± 0.001 was applied for muons produced by pion decay near the target. Counter 6 proved to be very useful in rejecting this process. Muons present in the incident beam contribute 0.971 ± 0.002. The corresponding correction factor at 92° is 0.998 ± 0.001.

A choice of a particular pulse-height region as that in which all hydrogen-scattered pions were to be found introduced some error at 163.5°. At 66° and 92°,

TABLE I. The uncorrected data.

Experimental period	Scattering angle (c.m.)	Number of particles incident on full target	Number of particles incident on empty target	Beam contamination	Hydrogen events per million incident
1	92°	10.5×10^6	5.0×10^6	0.045 ± 0.005	12.28 ± 1.75
2	92°	13.0×10^6	6.0×10^6	0.045 ± 0.005	12.90 ± 1.53
3	66°	13.5×10^6	8.2×10^6	0.080 ± 0.005	13.20 ± 1.94
4	66°	17.5×10^6	10.5×10^6	0.045 ± 0.005	11.93 ± 1.58
5	163.5°	5.2×10^6	3.5×10^6	0.120 ± 0.020	8.70 ± 3.10
6	163.5°	5.0×10^6	4.0×10^6	0.083 ± 0.020	8.15 ± 2.12
7	163.5°	17.3×10^6	9.0×10^6	0.070 ± 0.020	9.79 ± 1.38

TABLE II. Correction factors applied to the data.

	66°	92°	163.5°
Finite angular resolution	0.9996 ± 0.0001	0.9988 ± 0.0004	1.0040 ± 0.0004
Finite energy resolution	$0.993\ \pm0.002$	$1.000\ \pm0.0001$	0.9892 ± 0.0001
Random 12 coincidences		1.0020 ± 0.0005	at all angles
Decay of scattered pions into muons		$1.010\ \pm0.005$	at all angles
Absorption of pions after being recorded in counters 1 and 2		$1.008\ \pm0.001$	at all angles
Scattering from air in the empty target		$1.006\ \pm0.001$	at all angles

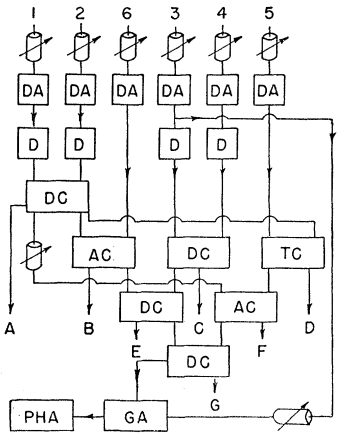

FIG. 5. Block diagram of the electronics. *DA* = distributed amplifier; *D* = discriminator; *DC* = diode coincidence circuit; *TC* = triode coincidence circuit; *AC* = anticoincidence circuit; *GA* = gated amplifier; *PHA* = pulse-height analyzer.

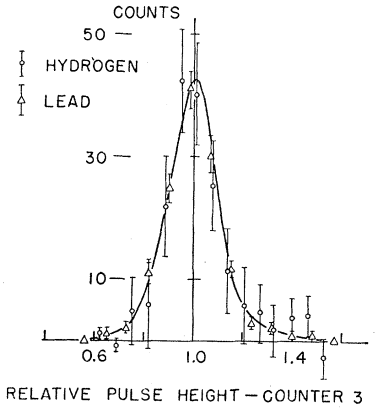

FIG. 6. Multiple scattering calibration at 66°.

multiple scattering from lead was used to define this region experimentally.[4] (See Figs. 6 and 7.)

B. The differential cross sections were calculated from the expression:

$$d\sigma/d\Omega = N_s/N_i N_t \Omega,$$

where N_s = number of scattered pions, N_i = number of incident particles, N_t = number of hydrogen atoms per cm² (the density of liquid hydrogen at 20.4°K was taken to be 0.0708 g/cm³), and Ω = solid angle.

The product $N_i N_t \Omega$ was evaluated and averaged over the distributed target. In performing this calculation, the experimental beam profile, the measured bowing of the target cup windows, and the variation of Ω as a function of position in the target were taken into account.

The results in the center-of-mass system at an energy of (24.8±2.3) Mev are:

Θ (deg)	$d\sigma/d\Omega$ (mb/sterad)
(66±9)	(0.286±0.028)
(92±9)	(0.458±0.042)
(163.5±7)	(0.993±0.120)

[4] L. Landau, J. Phys. U.S.S.R. 8, 201 (1944).

C. A least-squares phase-shift analysis has been performed with the aid of an IBM 650. We have chosen an approximate expression for the cross section in terms of three phase shifts[5]:

$$\frac{d\sigma}{d\Omega} = \lambda\!\!\!^{-2}\left\{\left|\frac{-n}{1-\cos\theta}+\alpha_3+(2\alpha_{33}+\alpha_{31})\cos\theta\right|^2 + (\alpha_{33}-\alpha_{31})^2\sin^2\theta\right\},$$

where α_3 is the phase shift for the S wave and α_{33} and α_{31} are the P-wave phase shifts for $J=\frac{3}{2}$ and $\frac{1}{2}$, respectively. The Coulomb parameter, n, is given by $n=e^2/\hbar v$, where v is the relative velocity of the particles. $\lambda\!\!\!^{-}$ is the reduced wavelength of the pion.

The phase shifts which result from this analysis still contain some non-nuclear portion. Van Hove has indicated[6] how the Born approximation to the Coulomb scattering amplitude may be improved by making corrections to the phase shifts to first order in n. This correction depends upon an assumption for the interaction radius. Our choice is the Compton wavelength of the pion. Now we may list the nuclear part of each phase shift with its associated standard deviation:

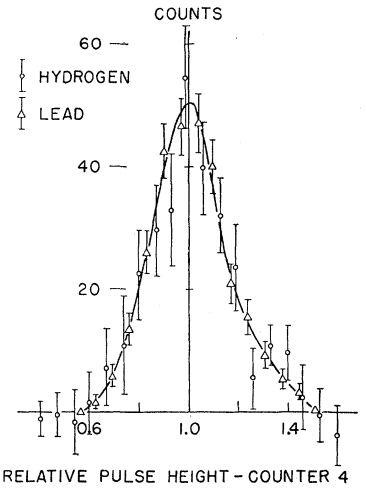

FIG. 7. Multiple scattering calibration at 92°.

$$-(3.23\pm0.42)^\circ=\alpha_3,$$
$$(2.05\pm0.39)^\circ=\alpha_{33},$$
$$-(0.47\pm0.41)^\circ=\alpha_{31},$$

These measurements have contributed to a detailed study of the energy dependence of the phase shifts. The results appear elsewhere.

[5] H. A. Bethe and F. deHoffmann, *Mesons and Fields* (Row, Peterson and Company, Evanston, 1955), Vol. II.

[6] L. Van Hove, Phys. Rev. 88, 1358 (1952).